NMR at operational temperature for resonance assignments of a PET degrading enzyme

Valeria Gabrielli[1], Jelena Grga[1], Sabine Gavalda[2], Laura Perrot[2], Emmanuelle Boll[3,4], Guy Lippens[1,*], Cyril Charlier[1,*]

[1]Toulouse Biotechnology Institute (TBI), University of Toulouse, CNRS, INRAE, INSA Toulouse, 135 Avenue de Rangueil, 31077 Toulouse Cedex 04, France
[2]Carbios, Parc Cataroux – Bâtiment B80, 8 rue de la Grolière, 63100 Clermont-Ferrand, France
[3]CNRS EMR 9002 ─ Integrative Structural Biology, F-59000 Lille, France.
[4]Univ. Lille, Inserm, CHU Lille, Institut Pasteur de Lille UMR 1167 ─ RID-AGE ─ Risk Factors and Molecular Determinants of Aging-Related Diseases, F-59000 Lille, France.

Correspondence to: Guy Lippens (glippens@insa-toulouse.fr) and Cyril Charlier (charlier@insa-toulouse.fr)

Abstract.

PETases are enzymes that can break down the PET polymer in its constituent building blocks, and thereby recycle starting material for new high-quality plastics. NMR spectroscopy can help in the understanding and ultimately improvement of these PETases, but is always confronted with the lengthy step of acquisition and interpretation of triple resonance spectra for the spectral assignment. Here, we explore whether this step can be made more efficient by recording the spectra directly at high temperature, which also corresponds to more realistic working conditions for the enzyme. Taking the inactive variant of LCC^{ICCG} in which the Serine 165 has been replaced by an Alanine (LCC^{ICCG}-S165A) as an example, we evaluate spectral quality at 30°C and 50°C, and find that the latter condition greatly improves the Signal-to-Noise (S/N) ratio of the different spectra. As a result, we present an exhaustive backbone and side-chain assignment of LCC^{ICCG}-S165A based on a minimal set of triple resonance spectra acquired at 50°C, that can act as a basis for future work on bio-structural studies on this PETase.

1 Introduction

PET hydrolase (PETase) enzymes are hydrolases that can break down the ester linkages in polyethylene terephthalate (PET), a common plastic used in the manufacturing of beverage bottles, food containers or clothing fibers. By breaking down PET into its constituent monomers, terephthalate and ethylene glycol, they offer a promising avenue for recovery of the building blocks that are the starting material for pristine plastic with the same characteristics as the initial waste, and thereby are a promising approach to address plastic pollution (Tournier et al., 2023). In this rapidly evolving field, many naturally

occurring PETase enzymes have been screened and used for further engineering. While the initial steps of the development of new or improved PETases often involve molecular modeling and/or bioinformatics, the starting 3D structures that serve as input for these efforts mostly come from X-ray crystallography (Liu et al., 2023). In this field, solution biomolecular NMR has been used only recently, notably to characterize the interaction between the enzyme and small soluble substrates (Charlier et al., 2022; Hellesnes et al., 2023) or to characterize the catalytic histidine with its associated pKa value (Charlier et al., 2024). Recently, a solid state NMR study of the Tfcut2 enzyme embedded in a trehalose glass in the presence of nanoparticles (NPs) made of ^{13}C labeled PET oligomers equally added to our understanding of the PET:enzyme interaction and the biocatalytic mechanism of the hydrolase reaction (Falkenstein et al., 2023).

Derived from the Leaf-branch Compost Cutinase (LCC) (Sulaiman et al., 2012), a type I thermostable cutinase (Tournier et al., 2023), its quadruple mutant LCC^{ICCG} has shown promise for industrial application of plastic recycling (Arnal et al., 2023; Tournier et al., 2020). As nearly all engineered PETases published so far, LCC^{ICCG} was optimized based on its activity as well as its thermostability (T_m = 85.8ºC for LCC and 93.3ºC for LCC^{ICCG} at pH 8, both proteins without C-terminal His-tag). From an NMR standpoint, this high thermostability could be at least in theory be a significant advantage, as spectral recording at higher temperatures leads to faster tumbling of the enzyme and hence mimics a lower molecular weight species. This is already exploited for the acquisition of two-dimensional spectra of monoclonal antibodies (~150 kDa), where their thermostability allows spectral recording at 50°C (Rößler et al., 2020). With a molecular weight of ~27 kDa for the unlabeled LCC^{ICCG}, peak broadening does interfere with spectral quality, and TROSY NMR approaches (Pervushin et al., 1997) and possibly deuteration of the enzyme (Gardner and Kay, 1998; LeMaster, 1989) would be helpful to progress in the assignment. Except for intrinsically disordered proteins (IDPs), where the relevant τ_c parameter does not correlate with the MW of the protein, the size problem is a general constraint for NMR samples, and leads to an exponentially decreasing number of deposited assignments for proteins larger than 150 residues, and finally to no more than ~ 100 entries for proteins of the size of LCC and its derivatives (Klukowski et al., 2023).

We examine here the (dis)advantages of recording a set of 3D experiments directly at higher temperatures. Taking the inactive variant of LCC^{ICCG}, in which the catalytic serine is replace by alanine (LCC^{ICCG}-S165A), as an example, we compare spectra at 30°C, temperature where we obtained our first assignments (Charlier et al., 2022), and similar experiments recorded at 50°C. We find that the standard triple resonance experiments work better at 50°C, with an important gain in S/N and hence in spectral recording time. Based on these observations, we complete our previous backbone and side chain assignments, and extend them to the side chain carboxyl resonances of the asparagine or aspartic acid (Asx) and glutamine or glutamic acid (Glx) residues. With the assignments at 50°C in hand, a temperature series of simple 2D spectra gives access to the assignments at both lower (30°C) and higher (70°C), whereby the latter temperature corresponds to the operational industrial conditions (Arnal et al., 2023). Whereas this motivates us to start the assignment task for future LCC mutants immediately at higher temperature, it will be interesting to see whether the same strategy will be fruitful for other PET hydrolases. Indeed, the field of PET degrading enzymes is rapidly evolving, and many enzymes are currently optimized leading to hundreds of variants with high industrial potential. Although it remains to be seen whether the improved NMR

characteristics, we find for the LCC^{ICCG} enzyme do translate to other PETases, we expect a positive answer due to their favorable thermostability. The ease of implementation without additional deuteration and with a limited set of standard NMR experiments should favor the use of NMR in this industrial research project.

2 Materials and Methods

2.1 Protein expression and purification

LCC^{ICCG}-S165A was expressed and purified according to previous studies (Charlier et al., 2022, 2024).

2.2 NMR spectroscopy

All experiments recorded for backbone and side chains resonances assignment were collected at 50ºC on 800 MHz spectrometer equipped with a 5-mm cryoprobe with z pulsed field gradients. The sample contained 580 µM of ^{15}N-^{13}C labeled protein in 25 mM Tris-HCl buffer pH 7.5 with 100 mM NaCl. The data presented here were recorded using the Bruker library pulse sequences: 2D ^{1}H-^{15}N HSQC, HNCA, HNCACB, HNCO, hCCcoNH-TOCSY, HcccoNH-TOCSY and HCACO. All spectra were processed using Topspin 4.0.8 (Bruker Biospin). Spectral analysis, backbone and side chain assignments were performed manually using POKY (Lee et al., 2021).

Spectral dimensions for the HNCO experiments were 3622 Hz (F_1) x 2919 Hz (F_2) x 12500 Hz (F_3) corresponding to 18 x 36 x 15.6224 ppm, with sampling durations of 15.5 ms (t_1), 10.9 ms (t_2), 160 ms (t_3). Spectra were centered at 4.700 ppm (^{1}H), 117.5 ppm (^{15}N), 173 ppm (^{13}CO). Spectral settings for the HNCA experiment were 6438.5 Hz (F_1) x 2919 Hz (F_2) x 12500 Hz (F_2) corresponding to 32 x 36 x 15.6224 ppm, with sampling durations of 14.9 ms (t_1), 10.9 ms (t_2), 150 ms (t_3). Spectra were centered at carriers were set to 4.7 ppm (^{1}H), 117.5 ppm (^{15}N), 54 ppm ($^{13}C\alpha$). Spectral settings for HNCACB only differs in the ^{13}C dimension with a spectral width of 14084.25 Hz corresponding to 50 ppm and 0.009 ms of acquisition time while the RF carrier was set to 40 ppm. All these experiments were acquired with 4 scans per increment. Side-chain assignment experiments Hcc(co)NH-TOCSY and hCC(co)NH-TOCSY were acquired with 8 and 16 scans per increment respectively. Spectral settings for the hCC(co)NH-TOCSY experiment were 14084.9 Hz (F_1) x 2919 Hz (F_2) x 12500 Hz (F_3) corresponding to 70.0044 x 36 x 15.6224 ppm, with sampling durations of 5.6 ms (t_1), 10.9 ms (t_2), 160 ms (t_3). Spectra were centered at carriers were set to 4.7 ppm (^{1}H), 117.5 ppm (^{15}N), 38 ppm (^{13}C). Spectral settings for the Hcc(co)NH-TOCSY experiment were 8001.337 Hz (F_1) x 2919 Hz (F_2) x 12500 Hz (F_2) corresponding to 10 x 36 x 15.6224 ppm, with sampling durations of 7.99 ms (t_1), 10.9 ms (t_2), 160 ms (t_3). Spectra were centered at carriers were set to 4.7 ppm (^{1}H), 117.5 ppm (^{15}N), 4.7 ppm (^{1}H). Spectral dimensions for the H(C)CO experiments were 6438.97 Hz (F_1) x 12500 Hz (F_2) corresponding to 32 x 15.6224 ppm, with sampling durations of 14.9 ms (t_1), 81.9 ms (t_2). Spectra were centered at carriers were set to 4.700 ppm (^{1}H), 39 ppm (^{13}C). Spectral dimensions for the HC (CO) experiments were 4426.42 Hz (F_1) x 12500 Hz (F_2)

corresponding to 22 x 15.6224 ppm, with sampling durations of 21.7 ms (t_1), 81.9 ms (t_2). RF carriers were set to 4.700 ppm (^{1}H), 40 ppm (^{13}C).

2.3 TRACT Analysis

TRACT spectra were recorded with the pulse sequence of Lee et al., implemented as individual experiments for the α and β ^{15}N spin states (Lee et al., 2006). A relaxation delay of 3s was used between scans, and 4k points were recorded. A total of 24 delays ranging from 1 to 200 ms were sampled as increments in a pseudo-2D matrix, and recorded with 512 scans per delay. After manual phasing and base line correction, the integral of the [10.0-6.4] ppm region was determined and plotted as a function of the corresponding delay. The resulting curve was fitted as a mono-exponentially decaying function, and the difference between the rates of both components was interpreted in terms of τ_c as described by Robson et al (Robson et al., 2021).

Theoretical calculus of the τ_c value as a function of temperature was performed by fixing the τ_c value at the experimentally determined value of 13ns for 30°C, and then applying the following formula (García De La Torre et al., 2000) :

$$\tau_c(30ºC) = \frac{\eta_{30ºC}}{\eta_T} * \frac{273 + T}{303} * \tau_c(T)$$

where η_T is the viscosity of water at the temperature T (using the Celsius scale). The latter was calculated using the equation from (Weast, 1979)

$$\eta_T = 1.7753 - 0.0565T + 1.0751 * 10^{-3}T^2 - 9.222 * 10^{-6}T^3$$

or, alternatively, from (Kestin et al., 1978):

$$log(\eta_T/\eta_{20}) = \frac{(20 - T)}{(T + 96)} \times 1.2378 - 1.303 * 10^{-3}(20 - T) + 3.06 * 10^{-6}(20 - T)^2 + 2.55 * 10^{-8}(20 - T)^3$$

and does not consider that our protein sample was not in pure water but rather in 25mM Tris-HCl and 100mM NaCl buffer pH 7.5.

3 Results

3.1 Comparative spectra at 30°C and 50°C

The global tumbling time τ_c (or, strictly speaking, the correlation time of the dipolar autocorrelation function of a given amide H-N vector) is one criterion that determines the linewidth of the corresponding amide correlation peak. Other factors such as chemical exchange of the amide protons with water or the presence of dynamics in the intermediate time scale

regime can equally contribute. Whereas the ratio of transverse (T_2) to longitudinal (T_1) relaxation times can be used to estimate this τ_c parameter (Tjandra et al., 1995), for larger proteins the increasing influence of intramolecular motions on the T_1 relaxation time (Luginbühl, 2002) has motivated the development of an alternative method. The dubbed TRACT (TRosy for rotAtional Correlation Times) method measures the decay of both TROSY and anti-TROSY components of the ^{15}N doublet (Lee et al., 2006), and translates the differential rate into a value of τ_c without interference of dipole–dipole (DD) relaxation by remote protons or relaxation contributions from chemical exchange (Lee et al., 2006; Robson et al., 2021). The TRACT experiments on the LCC^{ICCG}-S165A enzyme were recorded at various temperature ranging from 30ºC to 60ºC. By integrating the envelope of the proton spectra over the amide region as function of the relaxation delay, both relaxation rates were obtained using an exponential minimization (Figure 1. A & B). The difference between both rates (ΔR_2) was interpreted using the equation given by Robson and coauthors (Robson et al., 2021) and yielded τ_c values varying from 13 to 5.7 ns upon increasing the temperature from 30°C to 60°C (Figure 1. C). In agreement with the values expected from the temperature dependence of water viscosity for a rigid body of this size (García De La Torre et al., 2000) (Figure 1. D), this accelerated tumbling predicts a significant decrease in transverse relaxation rates for both amide and Cα resonances (Yamazaki et al., 1994), without the need for (partial) deuteration of the sample. We show here that because of this superior sensitivity, nearly complete assignment of the backbone and side chain spectra of LCC^{ICCG}-S165A can be obtained with a minimal set of experiments recorded at 50°C.

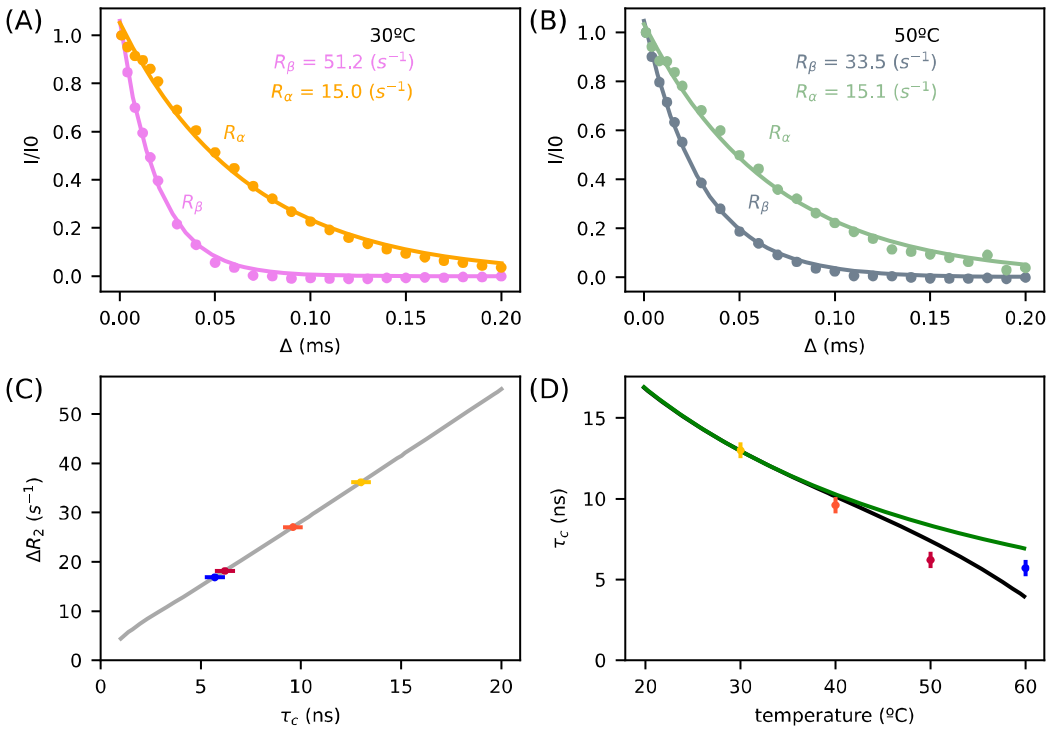

Figure 1. Determination of the correlation time τ_c as function of temperature. (**A-B**) TRACT analysis of LCC^{ICCG}-S165A at (**A**) 30ºC and (**B**) 50ºC. Both panels display the single-spin-state ^{15}N relaxation R_α and R_β decay curves obtained using the TRACT sequence. The dots represent the experimental points, and the lines represent the results of nonlinear regression of single exponential decay. (**C**) Theoretical curve of the difference between ^{15}N relaxation rates, ΔR_2 as function of τ_c following the equations of (Robson et al., 2021) (**D**) Theoretical curve of the temperature dependence of τ_c as predicted for a protein with its τ_c at 30°C fixed at 13 ns, based on the temperature dependence of water viscosity. On C and D panels, dots correspond to experimental values at 30ºC (yellow), 40ºC (orange), 50ºC (red) and 60ºC (blue). Solid lines shows the τ_c values as a function of temperature as calculated with water viscosity according to (Weast, 1979) (black) or (Kestin et al., 1978) (green). Error bars on (**C**) and (**D**) were calculated based on and estimated uncertainty of +/- 0.5 s^{-1} for the fits of the R_α and R_β curves.

To evaluate experimentally the influence of temperature on the spectral quality of our PETase, we recorded on the same sample at 30°C and 50°C both the ^{1}H-^{15}N HSQC and ^{1}H-^{15}N TROSY correlation spectra using standard Bruker pulse programs (*hsqcf3gpph19* and *trosyf3gpph19*). One important experimental factor we found is the necessity to seal the sample. Otherwise, already after a day, evaporation sets in and shim quality rapidly deteriorates. While we already observed at 30ºC an improved signal intensity by ~ 40% for the HSQC experiment compared to the TROSY, going to 50ºC clearly boosts the intensity gain by another ~15% (Figure 2.A). Equally important, the number of peaks in the 2D correlation spectra remains nearly the same between spectra recorded at both temperatures (Figure 2.B). Contrary to the case of IDPs, where amide proton signals at neutral to alkaline pH completely disappear at higher temperatures (Gil et al., 2013; Lopez et al., 2016), rapid amide proton exchange does not seem to represent a problem for this exceptionally stable PETase.

Building on this observation, we recorded tri-dimensional experiments at 30°C and 50ºC. In a typical backbone assignment experiment (*e.g.* HNCACB), the lengthy back-transfer of the $^{13}C\alpha$ to ^{15}N magnetization is often a limiting step due to the rapid transverse relaxation of the $^{13}C\alpha$ transverse magnetization. To evaluate how beneficial spectral recording at 50°C would be for LCC^{ICCG}, we first measured ^{1}H-^{13}C HMQC spectra with a wide ^{13}C spectral window both at 30ºC and 50ºC (Figure 2.C). Relative to the isolated methyl signal of M166 (Charlier et al., 2022), we observe a nearly 40% increase in intensity for $^{1}H\alpha$-$^{13}C\alpha$ resonances in the spectrum recorded at 50ºC compared to that at 30ºC. To evaluate the effect this has on triple resonance spectra, we acquired the ^{1}H-^{13}C planes of a HNCACB spectrum using the standard HSQC-based (*hncacbgpwg3d*) or TROSY-based (*trhncacbgp3d*) experiments both at 30ºC and 50ºC. Using a reasonable amount of spectrometer time (*e.g.* 8 scans per increment), the isolated $^{13}C\beta$ signals of threonine residues hardly come out of the noise at 30ºC while they are clearly visible at 50ºC (Figure 2.D). Although the use of the regular ^{1}H-^{15}N HSQC pulse sequence rather than its TROSY version was beneficial especially at 50°C (Figure 2. A & B), this advantage persists but becomes less pronounced in tri-dimensional experiments. Therefore, based on the results obtained so far, we recorded the full series of spectra for backbone and side chain assignment at 50°C with the regular triple resonance pulse sequences.

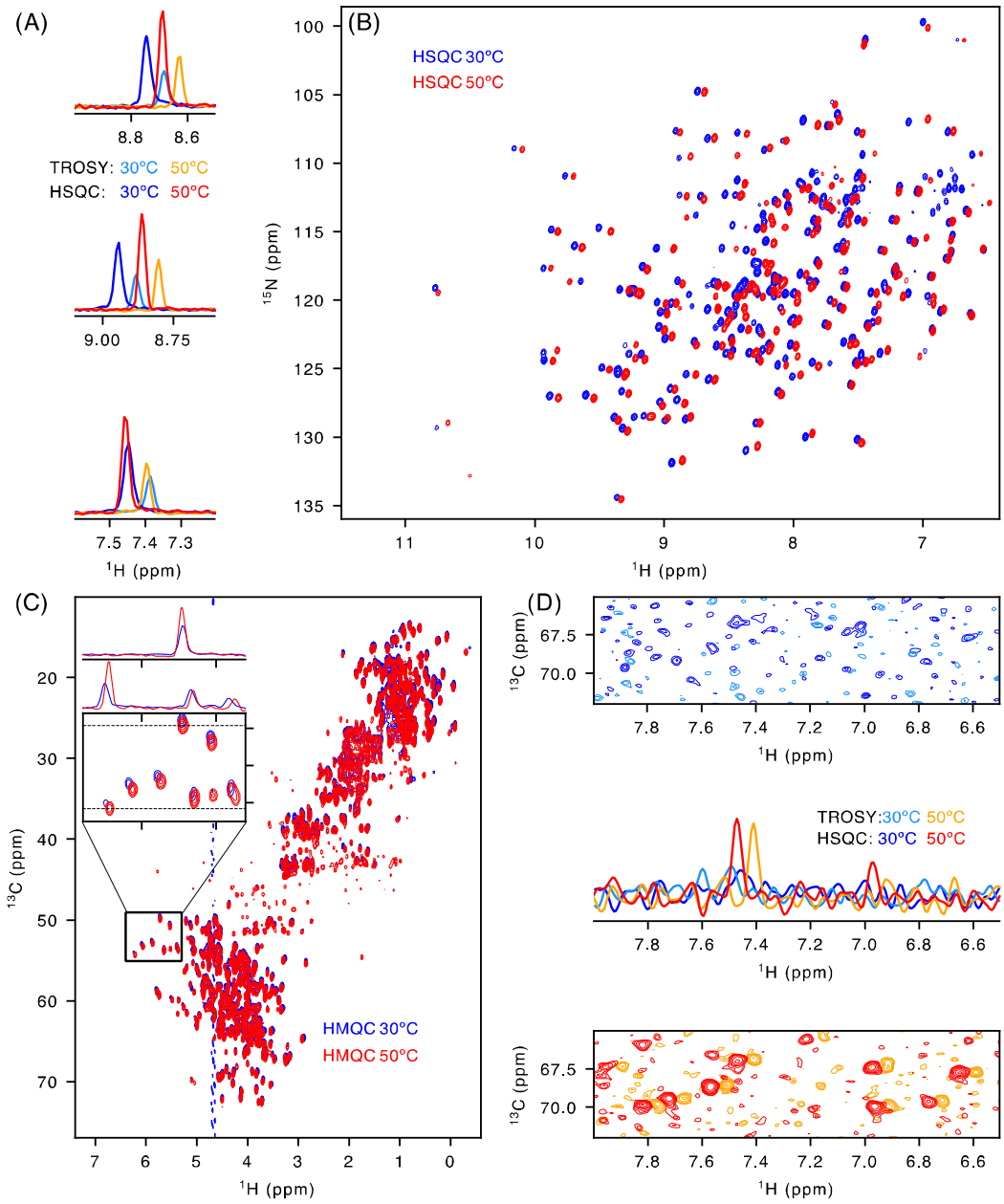

Figure 2: Selection of the best conditions and experiments for PETase assignment. (**A**) 1D ^{1}H slices through G88 (top), A59 (middle), G163 (bottom) cross peaks from ^{1}H-^{15}N TROSY at 30ºC (light-blue), ^{1}H-^{15}N TROSY at 50ºC (orange), ^{1}H-^{15}N HSQC at 30ºC (blue), ^{1}H-^{15}N HSQC at 50ºC (red). (**B**) ^{1}H-^{15}N HSQC at 30ºC (blue) and 50ºC (red). (**C**) ^{1}H-^{13}C HMQC at 30ºC (blue) and 50ºC (red). The insets show representative ^{13}Cα signals sharper at 50ºC compared to 30ºC. The ^{1}H 1D slices were taken at the ^{13}C frequency displayed by the dash lines at 50ºC and 30ºC. (**D**) Selected region of ^{1}H-^{13}C plane of HNCACB TROSY-based (light-blue) and HSQC-based (blue) at 30ºC (top) and of HNCACB TROSY-based (orange) and HSQC-based (red) at 50ºC (bottom). The central panel shows the 1D trace across one cross-peak near 7.4 ppm (^{1}H) and 67 ppm (^{13}C).

3.2 Backbone assignment

Figure 3 presents the assigned ^{1}H-^{15}N HSQC spectrum of LCC^{ICCG}-S165A based on only HNCA and HNCACB triple resonance spectra that were recorded at 50ºC and pH 7.5. The reported assignments follow the numbering of crystal structure (PDB code: 6tht) starting at Ser-36 and ending with Gln-293. Out of 258 amino acids, the expected number of backbone signals on this spectrum is 239 due to the presence of 18 prolines and the N-terminal Ser. We could assign 85% of the H-N resonances (Figure 3). A single loop between residues Ser-63 to Gly-73 connecting the N-terminal β1 and β2 strands could not be assigned. This loop is water exposed according to the crystal structure (PDB code: 6tht) and contains two Gly and three Ser residues, all factors that should promote rapid exchange with the solvent (Bai et al., 1993; Molday et al., 1972). Some other isolated N-H cross peaks, such as (Pro-43)-Asn-44-(Pro-45), could equally not be assigned. The completeness of the backbone assignment is nevertheless 85% for the ^{1}H^{N} and ^{15}N assignments (203 out of 239), 91% for ^{13}Cα (234 out of 258), 90% ^{13}Cβ (215 out of 239 residues, excluding the 19 glycines) and 85% of ^{13}C' (203 out of 239, excluding all residues preceding a Proline residue).

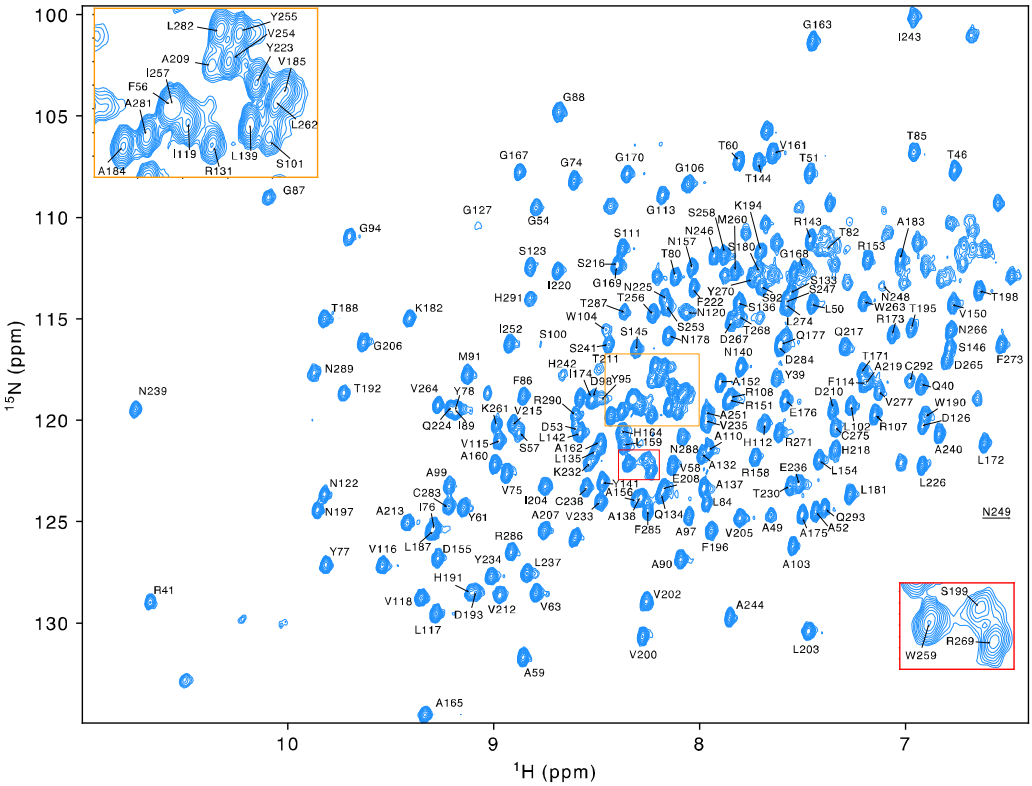

Figure 3: Two-dimensional ^{1}H-^{15}N HSQC spectrum of LCC^{ICCG}-S165A with residue-specific assignment at 50ºC. The crowded regions are represented in colored insets.

3.3 Extent of methyl assignment

In our effort to assign the side chain resonances, we first focused on methyl groups. LCC^{ICCG}-S165A contains 3 Met, 29 Ala, 9 Ile, 20 Val, 21 Leu, and 21 Thr residues, leading to a total of 153 methyl groups (3 Met-ε, 29 Ala-β, 9 Ile-δ1/Ile-γ2, 20 Val-γ1/Val-γ2, 21 Leu-δ1/Leu-δ2 and 21 Thr-γ2). Their assignment was carried out using two hCCcoNH-TOCSY and HcccoNH-TOCSY experiments acquired at 50ºC in 24 hours each. Non-uniform sampling could even further reduce this duration. In our previous work we had identified the three Met-ε resonances (Met-81, Met-166 and Met-260) using the absence of C-C coupling in the indirect dimension due to the neighboring sulfur atom in the side chain, and had assigned them through comparison with mutant enzymes and using a NOESY-based experiment (Charlier et al., 2022). All 29 Ala-β methyl groups were assigned both from the HNCACB experiment and from the following residue in the hCCcoNH/HcccoNH experiments. For isoleucine methyl groups, assignment was nearly complete, with the identification of 9 Ile-δ1 and 7 Ile-γ2 resonances (Figure 4). As Ile-220 is followed by Pro-221, preventing establishment of the connectivity from this residue, its Ile-δ1 resonance was assigned as the only remaining methyl with the specific ^{13}C chemical shift of isoleucine δ1 methyls. Valine residues contain 2 CH_3 groups which based on the spectra of our uniformly labeled protein cannot be distinguished (Gans et al., 2010). Overall, we assigned both Val-δ1 and Val-δ2 resonances for 12 Val residues, and a single methyl (by default called Val-δ1) for 3 Val residues. This leaves 5 Val that could not be assigned as they are followed either by a non-assigned residue (Ser-64, Ser-69 and Asn-278) or by proline residue (Pro-186 and Pro-201). Out of the 21 threonine residues we successfully assigned 13 Thr-γ2 signals out 16 resonances, leaving 5 Thr methyls unassigned as they are followed by non-assigned (Arg-47, Ser-83 and Gly-81) or by prolines residues (Pro-189 and Pro-231). For the three remaining threonines, only the ^{13}C-γ2 chemical shifts were obtained using the hCCcoNH-TOCSY. Finally, Leucines were the most incomplete methyl group assigned as we obtained the assignment of only 11 Leu with both Leu-δ1 and Leu-δ2 assigned. This is due to the proximity of the $^{13}C\delta1$, $^{13}C\delta2$ and $^{13}C\gamma$ resonances in the hCCcoNH-TOCSY and the fact that the CH_3 group of leucines fall into the most crowded region of the ^{1}H-^{13}C methyl spectra (Figure 4). Further assignment of leucines would probably require a lengthy 4D HCCcoNH-TOCSY experiment to directly connect the ^{13}C and ^{1}H resonances. Leucine specific labeling or a combination of mutants are other possible strategies (Gans et al., 2010; Plevin et al., 2011).

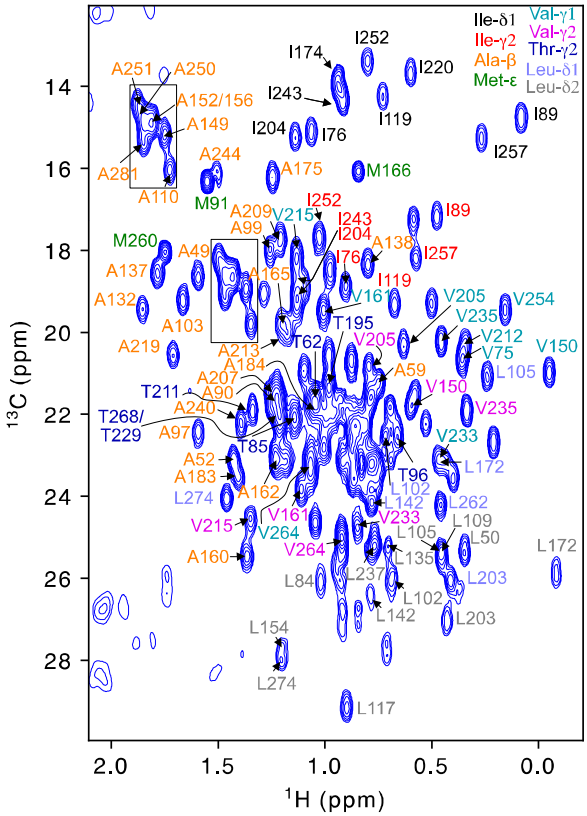

Figure 4: ^{1}H-^{13}C spectrum with labelled isolated methyl groups. Only isolated methyl signals were labelled and coloured based on their amino acid type. Assignment of methionines was based on our previous work (Charlier et al., 2022). For clarity reasons this spectrum is processed with a lower resolution in the indirect dimension to suppress the splitting in the indirect dimension due to the C-C coupling.

3.4 Assignment of Asx-Glx side chains

The flexibility of enzymes can also be approached through the dynamics of ^{13}Cδ/γ carbonyl or carboxyl functions of Asx of Glx residues (Engelke and Rüterjans, 1997; Hansen and Kay, 2011; Paquin et al., 2008; Stafford et al., 2013). These Asx and Glx residues are of prime importance in enzyme catalysis and more specifically in serine hydrolases that have an Asp in their catalytic triad (Everill et al., 2012). Even though the Asx/Glx residues represent nearly 20% of averaged bacterial proteins (Gerstein, 1997), the^{13}Cγ/δ of these nuclei are rarely assigned. Indeed, as of today (April 20th, 2024) only 1124 Asp-Cγ, 2949 Asn-Cγ, 1197 Glu-Cδ and 2944 Gln-Cδ chemical shifts are reported in the BMRB, representing only 2 to 8% of the number of assigned backbone carbonyl resonances of the same residues (51496, 35149, 67584 and 37917 respectively). The assignment of side chain carboxyl resonances was performed with a modified HCACO experiment (Kay et al., 1990). Originally developed for correlating intra-residue ^{1}Hα, ^{13}Cα, ^{13}C' resonances, this pulse sequence was latter optimized for the ^{13}C=O resonance of Asx/Glx side chains (Yamazaki et al., 1993). The use of 50ºC dramatically improved the quality of this HCACO like experiment. Figure 5 shows the H(C)CO and HC(CO) spectra used for the assignment at 50ºC.

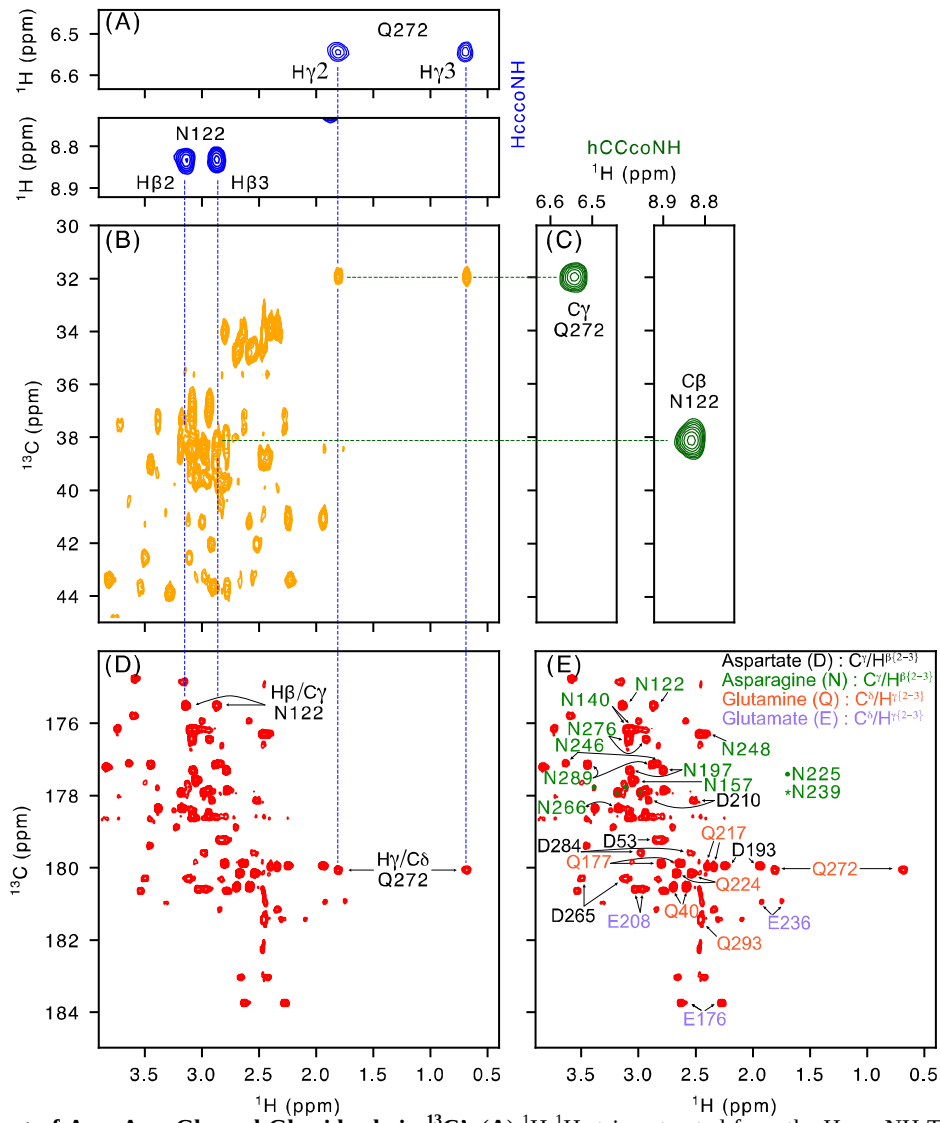

Figure 5: Assignment of Asp, Asn, Glu and Gln side chain ^{13}C'. (**A**) ^{1}H-^{1}H strip extracted from the HcccoNH-TOCSY experiment at the ^{15}N frequency of F273 (top) and S123 (bottom) and displaying the ^{1}Hγ resonances of Q272 (top) and ^{1}Hβ resonances of N122 (bottom). (**B**) HC(CO) spectrum correlating the methylene protons (Hγ or Hβ) and their attached carbon (Cγ or Cβ). (**C**) ^{1}H-^{13}C strip extracted from the hCCcoNH-TOCSY experiment at the ^{15}N frequency of F273 (left) and S123 (right) and displaying the ^{13}Cγ resonances of Q272 (left) and ^{13}Cβ resonances of N122 (right). (**D**) H(C)CO spectrum correlating the methylene protons (Hγ or Hβ) and their attached carboxyl (Cγ or Cδ). (**E**) H(C)CO spectrum with labeled assignments. Only N288 is not labeled as its signals are broad.

In the case of Asp and Asn residues the magnetization is transferred from ^{1}Hβ to ^{13}Cβ to ^{13}C'γ back and forth while for Glu and Gln residues the transfer starts from the ^{1}Hγ to ^{13}Cγ and finally to ^{13}Cδ. For instance, using the ^{1}H^{N}-^{1}H strip of the HcccoNH-TOCSY (Figure 5.A) and the ^{1}H^{N}-^{13}C strip of the hCCcoNH-TOCSY (Figure 5.C) both extracted at the ^{15}N frequency of a residue following an Asp or Asn residue, one can correlate Hβ(s) and Cβ resonances on HC(CO) experiment

(Figure 5.B). The same pathway was applied to Glu and Gln residues, but it now correlated the Hγ(s) and Cγ resonances. In at the H(C)CO spectrum (Figure 5.D) the ^{1}H frequencies align with the HC(CO) spectrum as they both start from the same protons. Using this procedure, we assigned 12 Asn ^{13}C'γ resonances (67%, 3 are followed by Prolines: Pro-38, Pro-45, Pro-179 and 3 by residues for which the backbone resonance is not assigned: Thr-121, Ala-250 and Asn-279), 5 Asp ^{13}Cγ resonances (45%, 1 is followed by a Proline: Pro-280, and 1 by non-assigned residue: Ser-130), 3 Glu ^{13}C'δ resonances (100 %) and 6 Gln (85%) ^{13}C'δ resonances (Figure 5.E).

Overall, the side-chain assignments presented above are based on a minimal set of three-dimensional experiments (from the Bruker library) combining the HNCACB (also used for backbone assignment) and the HcccoNH-TOCSY, hCCcoNH-TOCSY, HC(CO) (run as a 2D planes here). Many NMR studies of proteins of molecular weight of ~25 kDa and above struggle with the necessity to use of large set of sophisticated three- (and even higher) dimensional experiments. Although the use of methods to speed-up data acquisition (Non-Uniform Sampling, SO-FAST(Schanda et al., 2005)) can be very useful to further decrease the (precious and expensive) experimental time, they often require tweaking by experienced NMR spectroscopists. If NMR wants to find its place in such a large-scale project as the development of industrial PETases, easy, rapid and robust methods providing side-specific information are essential.

4 Conclusions

Although much recent progress has been made in the assignment of proteins, it remains a potential bottleneck of many projects in which NMR is involved. This is particularly true for enzymes that are near or beyond the size-limit of solution state NMR. Type I thermostable hydrolases such as LCC are in this size range, and although their NMR assignment clearly cannot keep up with the many variants that are tested in academic and industrial laboratories all over the world, speeding up the process would increase its use in this rapidly evolving field. Studying these enzymes in what we would call 'near-working conditions" (Arnal et al., 2023) (to make the parallel with "near-physiological conditions" for disease related enzymes) implies to study them at high temperature. For solution state NMR, we have demonstrated here that this is a win-win situation, as the rotational correlation time associated with the molecular weight of the protein (~27 kDa) is drastically reduced by working at 50ºC, allowing efficient magnetization transfer and hence high-quality triple resonance spectra. 50ºC was chosen as an intermediate temperature between room temperature and the operational conditions. Acquiring data at even higher temperature is feasible with precautions as hydrogen exchange and stability of enzyme(s) over time could become an issue along with technical issues as we are approaching the limit of cryoprobes. The resulting completeness of the assignment with a minimal set of experiments is quite satisfactory, as we show here for the LCC^{ICCG} inactive variant. The additional methyl groups, other side chain ^{13}C resonances and side chain carboxyl resonances obtained with the help of the spectra at 50°C indeed complete the NMR picture of LCC^{ICCG}-S165A (Figure 6). It is important to point out that all the backbone and side-chain assignments presented here were obtained using doubly labeled sample in H_2O. This approach

facilitates the sample preparation and significantly decreases the price of samples compared to more sophisticated approaches requiring deuteration for instance. Although His imidazole ring resonances have been reported recently (Charlier et al., 2024), the side chain resonances of aromatic amino acids: Tyr, Phe, Trp have not been assigned yet as they require specific experiments (Prompers et al., 1998; Shukla et al., 2024) that should however equally profit from measurement at 50°C. The complete set of ^{1}H and ^{13}C assignments reported here establishes the basis for future NMR work on these PET hydrolase enzymes at the forefront of the battle against plastic pollution.

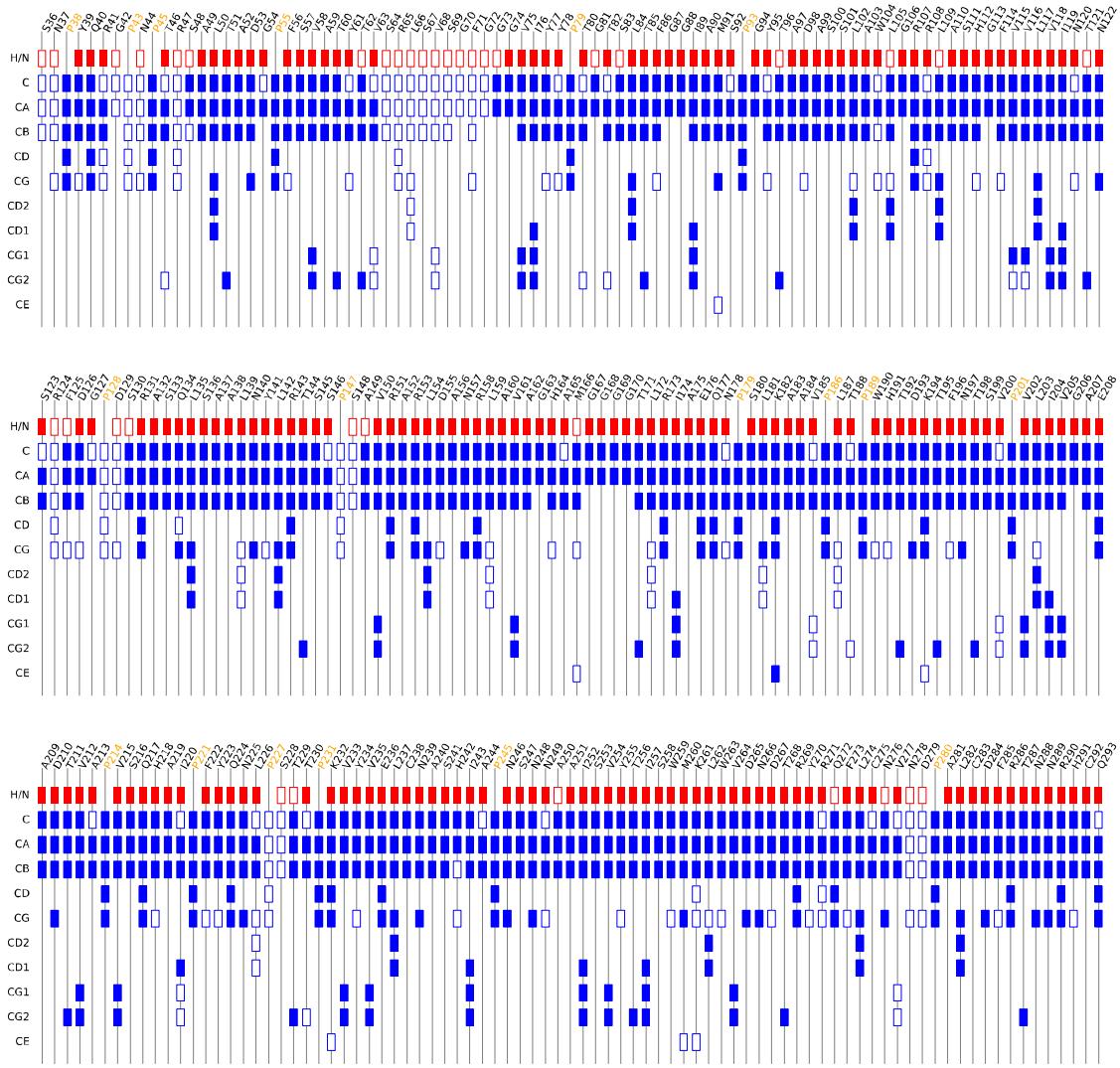

Figure 6: Diagram representing the completeness of H/N backbone and C assignments. For each residue a vertical line represents

the chain with in red the amide moity (H/N) and in blue all the carbons of the backbone and side chain. For each atom present in the chain a rectangle is represented. Filled rectangle means that the resonance has been assigned and, at the opposite, empty rectangle means that this resonance has not been assigned. Cζ or Arg; Cδ1, Cδ2, Cε1, Cε2, Cζ for Tyr; Cδ2 and Cε1 for His; Cδ1, Cδ2, Cε2, Cε3, Cζ2, Cζ3 and Cη2 for Trp; and Cδ2, Cδ1, Cε1, Cε2, Cζ for Phe were removed from this list as they cannot be assigned by our experimental series.

Author Contributions

VG and **EB** analysed backbone and side chain spectra; **JG, LP** and **SG** Resources; **GL & CC** Conceptualization, Project administration, Supervision, Writing – original draft preparation, Writing - review & editing. All authors reviewed the manuscript.

Acknowledgements

We would like to thank Alain Marty, Vincent Tournier, Nicolas Chabot, and Marc Gueroult (Carbios, France) for insightful discussions and comments on the manuscript. We thank the ICEO facility of the Toulouse Biotechnology Institute (TBI), which is part of the Integrated Screening Platform of Toulouse (PICT, IBiSA), for providing access to protein-purification equipment. We thank Dr. E. Cahoreau and L. Peyriga in the MetaToul (Toulouse metabolomics & fluxomics facilities, www.metatoul.fr) NMR facility. MetaToul is part of the French National Infrastructure for Metabolomics and Fluxomics MetaboHUB-AR-11-INBS-0010 (www.metabohub.fr), and is supported by the Région Midi-Pyrénées, the ERDF, the SICOVAL and the French Minister of Education & Research, who are all gratefully acknowledged. We thank Dr. FX Cantrelle (Lille, France) for insightful discussions. Financial support from the IR INFRANALYTICS FR2054 for conducting the research is gratefully acknowledged. This study was supported by the OPTIZYME grant financed by ADEME - contract number 2282D0513-C.

Declaration of interest

L.P. and S.G. are employees of Carbios. All other authors declare no competing interests.

Data availability

Chemical shifts are submitted to the BMRB with the accession number 52519.

NMR spectra have been deposited to https://doi.org/10.5281/zenodo.11349991. All the data used in figure 1, the assignment experiment (HNCA, HNCACB, HNCO, hCCcoNH-TOCSY and HCCcoNH-TOCSY) and both planes of HCACO experiments.

References

Arnal, G., Anglade, J., Gavalda, S., Tournier, V., Chabot, N., Bornscheuer, U. T., Weber, G., and Marty, A.: Assessment of Four Engineered PET Degrading Enzymes Considering Large-Scale Industrial Applications, ACS Catal., 13156–13166, https://doi.org/10.1021/acscatal.3c02922, 2023.

Bai, Y., Milne, J. S., Mayne, L., and Englander, S. W.: Primary structure effects on peptide group hydrogen exchange, Proteins, 17, 75–86, https://doi.org/10.1002/prot.340170110, 1993.

Charlier, C., Gavalda, S., Borsenberger, V., Duquesne, S., Marty, A., Tournier, V., and Lippens, G.: An NMR look at an engineered PET depolymerase, Biophysical Journal, 121, 2882–2894, https://doi.org/10.1016/j.bpj.2022.07.002, 2022.

Charlier, C., Gavalda, S., Grga, J., Perrot, L., Gabrielli, V., Löhr, F., Schörghuber, J., Lichtenecker, R., Arnal, G., Marty, A., Tournier, V., and Guy, L.: Exploring the pH dependence of an improved PETase, Biophysical Journal, S0006349524002881, https://doi.org/10.1016/j.bpj.2024.04.026, 2024.

Engelke, J. and Rüterjans, H.: Backbone dynamics of proteins derived from carbonyl carbon relaxation times at 500, 600 and 800 MHz: Application to ribonuclease T1, Journal of Biomolecular NMR, 9, 63–78, https://doi.org/10.1023/A:1018675618785, 1997.

Everill, P., Sudmeier, J. L., and Bachovchin, W. W.: Direct NMR Observation and p K_a Determination of the Asp ^{102} Side Chain in a Serine Protease, J. Am. Chem. Soc., 134, 2348–2354, https://doi.org/10.1021/ja210091q, 2012.

Falkenstein, P., Zhao, Z., Di Pede-Mattatelli, A., Künze, G., Sommer, M., Sonnendecker, C., Zimmermann, W., Colizzi, F., Matysik, J., and Song, C.: On the Binding Mode and Molecular Mechanism of Enzymatic Polyethylene Terephthalate Degradation, ACS Catal., 13, 6919–6933, https://doi.org/10.1021/acscatal.3c00259, 2023.

Gans, P., Hamelin, O., Sounier, R., Ayala, I., Durá, M. A., Amero, C. D., Noirclerc□Savoye, M., Franzetti, B., Plevin, M. J., and Boisbouvier, J.: Stereospecific Isotopic Labeling of Methyl Groups for NMR Spectroscopic Studies of High□Molecular□Weight Proteins, Angew Chem Int Ed, 49, 1958–1962, https://doi.org/10.1002/anie.200905660, 2010.

García De La Torre, J., Huertas, M. L., and Carrasco, B.: HYDRONMR: Prediction of NMR Relaxation of Globular Proteins from Atomic-Level Structures and Hydrodynamic Calculations, Journal of Magnetic Resonance, 147, 138–146, https://doi.org/10.1006/jmre.2000.2170, 2000.

Gardner, K. H. and Kay, L. E.: The use of 2H, 13C, 15N multidimensional NMR to study the structure and dynamics of proteins, Annu Rev Biophys Biomol Struct, 27, 357–406, https://doi.org/10.1146/annurev.biophys.27.1.357, 1998.

Gerstein, M.: A structural census of genomes: comparing bacterial, eukaryotic, and archaeal genomes in terms of protein structure, Journal of Molecular Biology, 274, 562–576, https://doi.org/10.1006/jmbi.1997.1412, 1997.

Gil, S., Hošek, T., Solyom, Z., Kümmerle, R., Brutscher, B., Pierattelli, R., and Felli, I. C.: NMR Spectroscopic Studies of Intrinsically Disordered Proteins at Near Physiological Conditions, Angew Chem Int Ed, 52, 11808–11812, https://doi.org/10.1002/anie.201304272, 2013.

Hansen, A. L. and Kay, L. E.: Quantifying millisecond time-scale exchange in proteins by CPMG relaxation dispersion NMR spectroscopy of side-chain carbonyl groups, J Biomol NMR, 50, 347–355, https://doi.org/10.1007/s10858-011-9520-6, 2011.

Hellesnes, K. N., Vijayaraj, S., Fojan, P., Petersen, E., and Courtade, G.: Biochemical Characterization and NMR Study of a PET-Hydrolyzing Cutinase from *Fusarium solani pisi*, Biochemistry, 62, 1369–1375, https://doi.org/10.1021/acs.biochem.2c00619, 2023.

Joo, S., Cho, I. J., Seo, H., Son, H. F., Sagong, H.-Y., Shin, T. J., Choi, S. Y., Lee, S. Y., and Kim, K.-J.: Structural insight into molecular mechanism of poly(ethylene terephthalate) degradation, Nat Commun, 9, 382, https://doi.org/10.1038/s41467-018-02881-1, 2018.

Kay, L. E., Ikura, M., Tschudin, R., and Bax, A.: Three-dimensional triple-resonance NMR spectroscopy of isotopically enriched proteins, Journal of Magnetic Resonance (1969), 89, 496–514, https://doi.org/10.1016/0022-2364(90)90333-5, 1990.

Kestin, J., Sokolov, M., and Wakeham, W. A.: Viscosity of liquid water in the range −8 °C to 150 °C, Journal of Physical and Chemical Reference Data, 7, 941–948, https://doi.org/10.1063/1.555581, 1978.

Klukowski, P., Riek, R., and Güntert, P.: Time-optimized protein NMR assignment with an integrative deep learning approach using AlphaFold and chemical shift prediction, Sci. Adv., 9, eadi9323, https://doi.org/10.1126/sciadv.adi9323, 2023.

Lee, D., Hilty, C., Wider, G., and Wüthrich, K.: Effective rotational correlation times of proteins from NMR relaxation interference, Journal of Magnetic Resonance, 178, 72–76, https://doi.org/10.1016/j.jmr.2005.08.014, 2006.

Lee, W., Rahimi, M., Lee, Y., and Chiu, A.: POKY: a software suite for multidimensional NMR and 3D structure calculation of biomolecules, Bioinformatics, 37, 3041–3042, https://doi.org/10.1093/bioinformatics/btab180, 2021.

LeMaster, D. M.: [2] Deuteration in protein proton magnetic resonance, in: Methods in Enzymology, vol. 177, Academic Press, 23–43, https://doi.org/10.1016/0076-6879(89)77004-X, 1989.

Liu, F., Wang, T., Yang, W., Zhang, Y., Gong, Y., Fan, X., Wang, G., Lu, Z., and Wang, J.: Current advances in the structural biology and molecular engineering of PETase, Front. Bioeng. Biotechnol., 11, 1263996, https://doi.org/10.3389/fbioe.2023.1263996, 2023.

Lopez, J., Schneider, R., Cantrelle, F., Huvent, I., and Lippens, G.: Studying Intrinsically Disordered Proteins under True In Vivo Conditions by Combined Cross□Polarization and Carbonyl□Detection NMR Spectroscopy, Angew Chem Int Ed, 55, 7418–7422, https://doi.org/10.1002/anie.201601850, 2016.

Luginbühl, P.: Semi-classical nuclear spin relaxation theory revisited for use with biological macromolecules, Progress in Nuclear Magnetic Resonance Spectroscopy, 40, 199–247, https://doi.org/10.1016/S0079-6565(01)00043-7, 2002.

Molday, R. S., Englander, S. W., and Kallen, R. G.: Primary structure effects on peptide group hydrogen exchange, Biochemistry, 11, 150–158, https://doi.org/10.1021/bi00752a003, 1972.

Paquin, R., Ferrage, F., Mulder, F. A. A., Akke, M., and Bodenhausen, G.: Multiple-Timescale Dynamics of Side-Chain Carboxyl and Carbonyl Groups in Proteins by ^{13}C Nuclear Spin Relaxation, J. Am. Chem. Soc., 130, 15805–15807, https://doi.org/10.1021/ja803794g, 2008.

Pervushin, K., Riek, R., Wider, G., and Wüthrich, K.: Attenuated T_2 relaxation by mutual cancellation of dipole–dipole coupling and chemical shift anisotropy indicates an avenue to NMR structures of very large biological macromolecules in solution, Proc. Natl. Acad. Sci. U.S.A., 94, 12366–12371, https://doi.org/10.1073/pnas.94.23.12366, 1997.

Plevin, M. J., Hamelin, O., Boisbouvier, J., and Gans, P.: A simple biosynthetic method for stereospecific resonance assignment of prochiral methyl groups in proteins, J Biomol NMR, 49, 61–67, https://doi.org/10.1007/s10858-010-9463-3, 2011.

Prompers, J. J., Groenewegen, A., Hilbers, C. W., and Pepermans, H. A. M.: Two-Dimensional NMR Experiments for the Assignment of Aromatic Side Chains in13C-labeled Proteins, Journal of Magnetic Resonance, 130, 68–75, https://doi.org/10.1006/jmre.1997.1277, 1998.

Robson, S. A., Dağ, Ç., Wu, H., and Ziarek, J. J.: TRACT revisited: an algebraic solution for determining overall rotational correlation times from cross-correlated relaxation rates, J Biomol NMR, 75, 293–302, https://doi.org/10.1007/s10858-021-00379-5, 2021.

Rößler, P., Mathieu, D., and Gossert, A. D.: Enabling NMR Studies of High Molecular Weight Systems Without the Need for Deuteration: The XL□ALSOFAST Experiment with Delayed Decoupling, Angew Chem Int Ed, 59, 19329–19337, https://doi.org/10.1002/anie.202007715, 2020.

Schanda, P., Kupče, Ē., and Brutscher, B.: SOFAST-HMQC Experiments for Recording Two-dimensional Deteronuclear Correlation Spectra of Proteins within a Few Seconds, J Biomol NMR, 33, 199–211, https://doi.org/10.1007/s10858-005-4425-x, 2005.

Shukla, V. K., Karunanithy, G., Vallurupalli, P., and Hansen, D. F.: Characterising Aromatic Side Chains in Proteins through the Synergistic Development of NMR Experiments and Deep Neural Networks, https://doi.org/10.1101/2024.04.01.587635, 2 April 2024.

Stafford, K. A., Ferrage, F., Cho, J.-H., and Palmer, A. G.: Side Chain Dynamics of Carboxyl and Carbonyl Groups in the Catalytic Function of *Escherichia coli* Ribonuclease H, J. Am. Chem. Soc., 135, 18024–18027, https://doi.org/10.1021/ja409479y, 2013.

Sulaiman, S., Yamato, S., Kanaya, E., Kim, J.-J., Koga, Y., Takano, K., and Kanaya, S.: Isolation of a Novel Cutinase Homolog with Polyethylene Terephthalate-Degrading Activity from Leaf-Branch Compost by Using a Metagenomic Approach, Appl Environ Microbiol, 78, 1556–1562, https://doi.org/10.1128/AEM.06725-11, 2012.

Tjandra, N., Feller, S. E., Pastor, R. W., and Bax, A.: Rotational diffusion anisotropy of human ubiquitin from 15N NMR relaxation, J. Am. Chem. Soc., 117, 12562–12566, https://doi.org/10.1021/ja00155a020, 1995.

Tournier, V., Topham, C. M., Gilles, A., David, B., Folgoas, C., Moya-Leclair, E., Kamionka, E., Desrousseaux, M.-L., Texier, H., Gavalda, S., Cot, M., Guémard, E., Dalibey, M., Nomme, J., Cioci, G., Barbe, S., Chateau, M., André, I., Duquesne, S., and Marty, A.: An engineered PET depolymerase to break down and recycle plastic bottles, Nature, 580, 216–219, https://doi.org/10.1038/s41586-020-2149-4, 2020.

Tournier, V., Duquesne, S., Guillamot, F., Cramail, H., Taton, D., Marty, A., and André, I.: Enzymes' Power for Plastics Degradation, Chem. Rev., 123, 5612–5701, https://doi.org/10.1021/acs.chemrev.2c00644, 2023.

Weast, R. C. (Ed.): CRC handbook of chemistry and physics. A ready-reference book of chemical and physical data, 59. ed., CRC P, Boca Raton, 2492 pp., 1979.

Yamazaki, T., Yoshida, M., and Nagayama, K.: Complete assignments of magnetic resonances of ribonuclease H from Escherichia coli by double- and triple-resonance 2D and 3D NMR spectroscopies, Biochemistry, 32, 5656–5669, https://doi.org/10.1021/bi00072a023, 1993.

Yamazaki, T., Lee, W., Arrowsmith, C. H., Muhandiram, D. R., and Kay, L. E.: A Suite of Triple Resonance NMR Experiments for the Backbone Assignment of 15N, 13C, 2H Labeled Proteins with High Sensitivity, J. Am. Chem. Soc., 116, 11655–11666, https://doi.org/10.1021/ja00105a005, 1994.

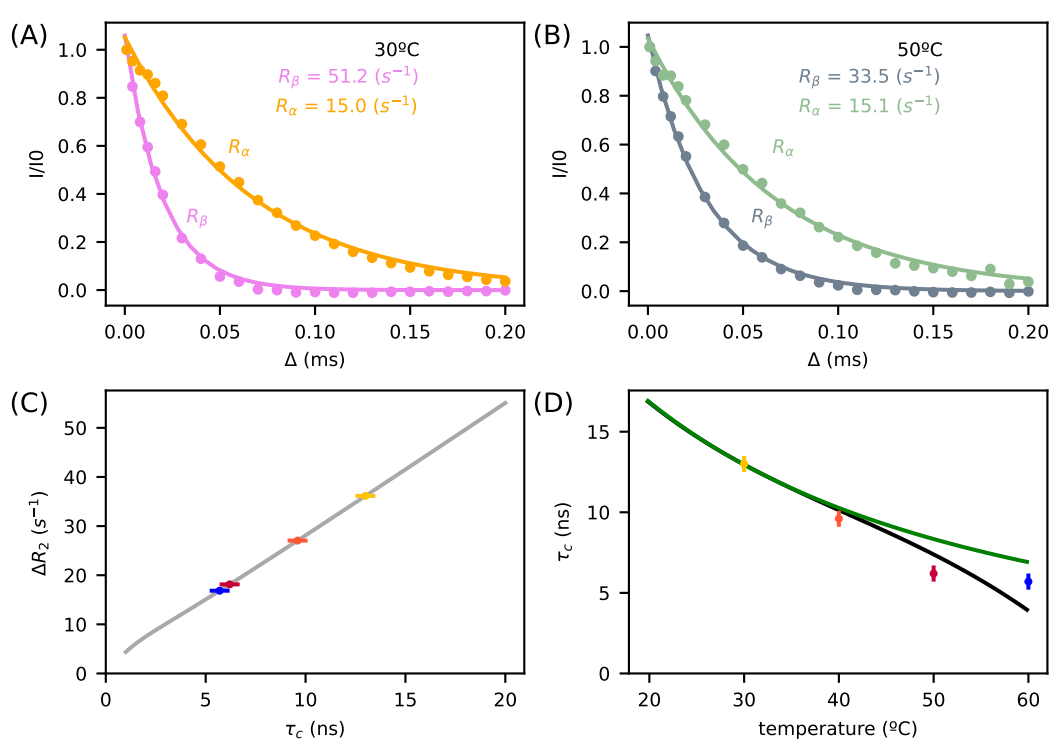
(A)
30ºC
R_β = 51.2 (s^{-1})
R_α = 15.0 (s^{-1})
R_α
R_β
I/I0
Δ (ms)
(B)
50ºC
R_β = 33.5 (s^{-1})
R_α = 15.1 (s^{-1})
R_α
R_β
I/I0
Δ (ms)
(C)
ΔR_2 (s^{-1})
τ_c (ns)
(D)
τ_c (ns)
temperature (ºC)

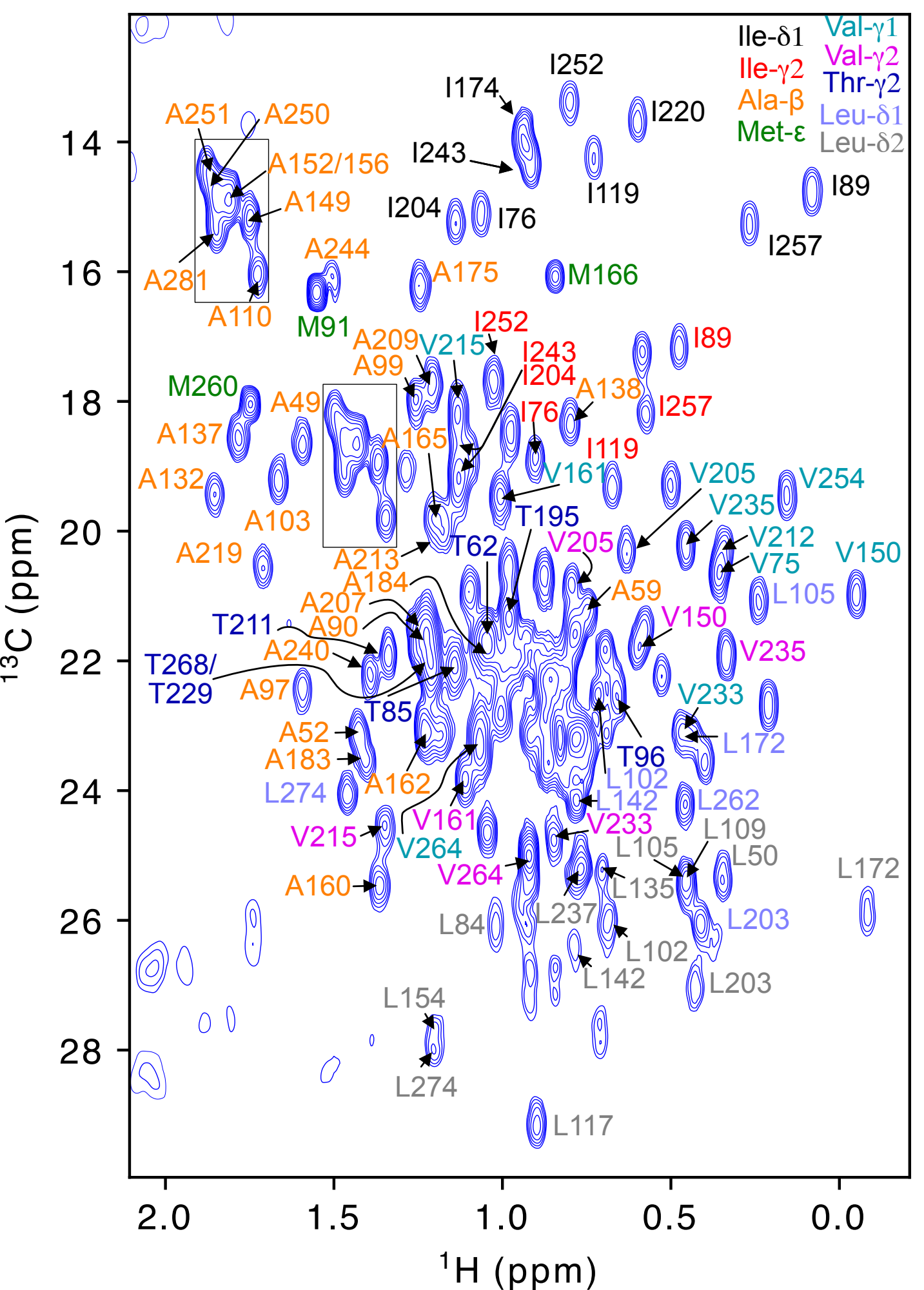

Ile-δ1
Ile-γ2
Ala-β
Met-ε
Val-γ1
Val-γ2
Thr-γ2
Leu-δ1
Leu-δ2
A251
A250
A152/156
A149
A281
A110
A244
M91
I174
I252
I220
I243
I119
I204
I76
I89
I257
A175
M166
I252
A209
V215
I243
I204
A99
I89
M260
A49
A138
I257
A137
A165
I76
I119
A132
V161
V205
V254
V235
A103
T195
V212
A219
A213
T62
V205
V75
V150
A184
A59
L105
A207
T211
A90
V150
A240
V235
T268/
T229
A97
T85
V233
A52
L172
A183
T96
L102
L274
A162
L142
L262
V161
V233
V215
V264
L109
L105
L50
V264
L172
A160
L135
L237
L84
L203
L102
L142
L203
L154
L274
L117
14
16
18
20
22
24
26
28
2.0
1.5
1.0
0.5
0.0
^{13}C (ppm)
^{1}H (ppm)

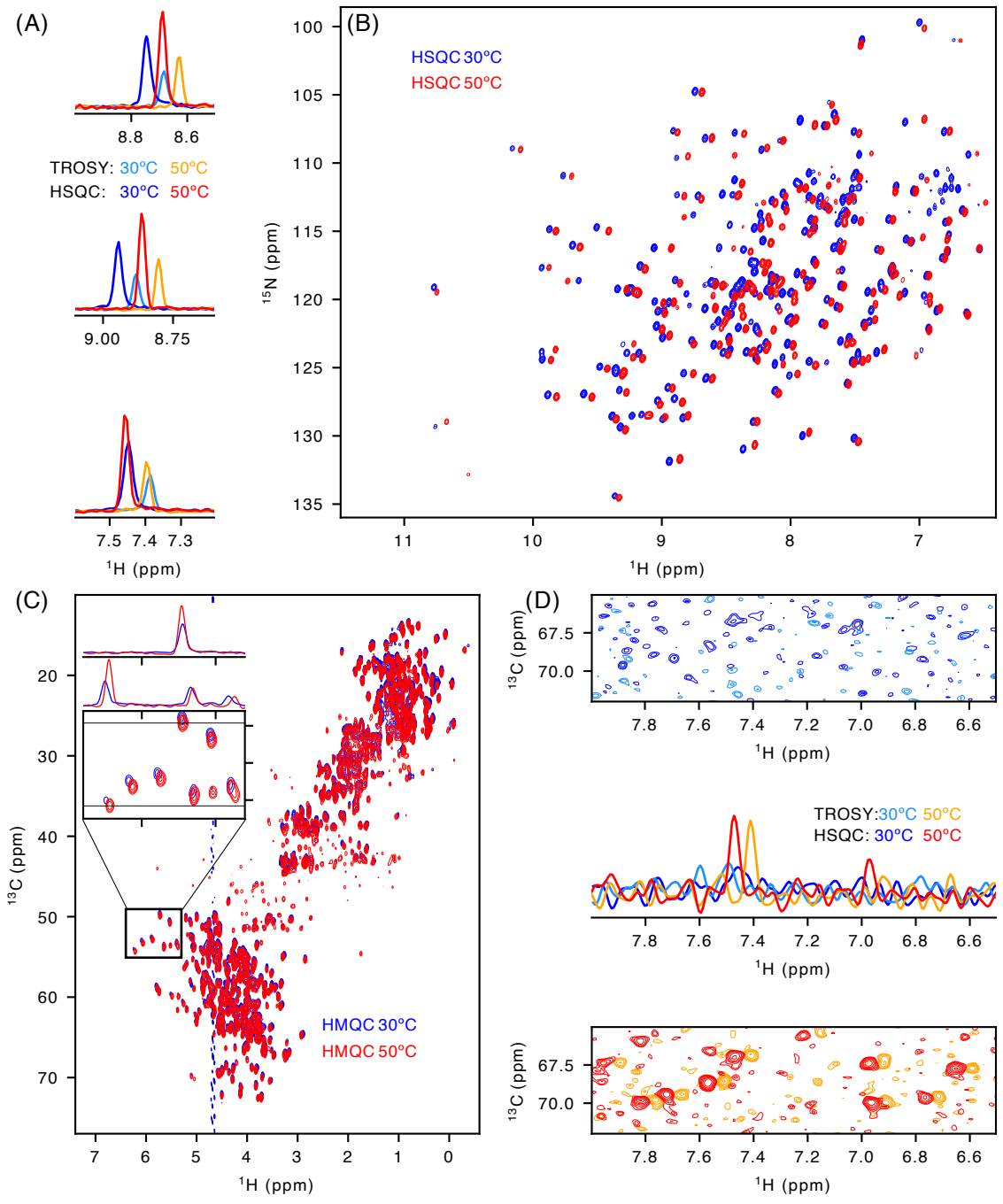
(A)
8.8
8.6
TROSY: 30°C 50°C
HSQC: 30°C 50°C
9.00
8.75
7.5 7.4 7.3
^{1}H (ppm)
(B)
HSQC 30°C
HSQC 50°C
^{15}N (ppm)
^{1}H (ppm)
(C)
^{13}C (ppm)
HMQC 30°C
HMQC 50°C
^{1}H (ppm)
(D)
^{13}C (ppm)
^{1}H (ppm)
TROSY:30°C 50°C
HSQC: 30°C 50°C

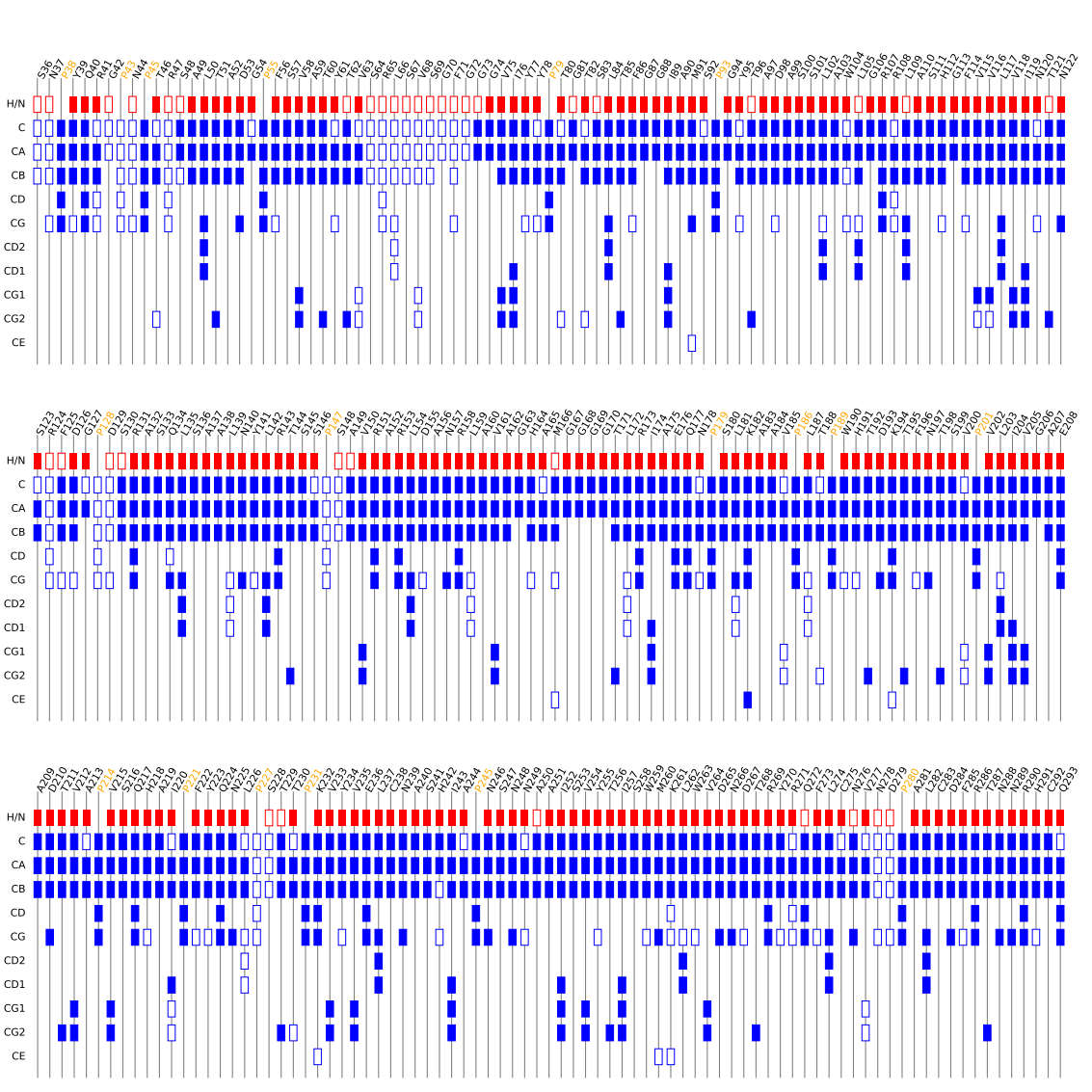
S36 R37 P38 Y39 Q40 R41 G42 P43 N44 P45 T46 R47 S48 A49 L50 T51 A52 D53 G54 P55 F56 S57 V58 A59 T60 Y61 T62 V63 S64 R65 L66 S67 V68 S69 G70 F71 G72 G73 G74 V75 T76 V77 V78 P79 T80 G81 T82 S83 L84 T85 R86 G87 G88 I89 A90 M91 S92 P93 G94 Y95 T96 A97 D98 A99 S100 S101 L102 A103 W104 L105 G106 R107 R108 L109 A110 S111 H112 G113 F114 V115 V116 L117 V118 I119 N120 T121 N122
H/N
C
CA
CB
CD
CG
CD2
CD1
CG1
CG2
CE
S123 R124 F125 D126 G127 P128 D129 S130 R131 A132 S133 Q134 L135 S136 A137 A138 L139 N140 Y141 L142 R143 T144 S145 S146 P147 S148 A149 V150 R151 A152 R153 L154 D155 A156 N157 R158 L159 A160 V161 A162 G163 H164 A165 M166 G167 G168 G169 G170 T171 L172 R173 I174 A175 E176 Q177 N178 P179 S180 L181 K182 A183 A184 V185 P186 L187 T188 P189 W190 H191 T192 D193 K194 T195 F196 N197 T198 S199 V200 P201 V202 L203 I204 V205 G206 A207 E208
H/N
C
CA
CB
CD
CG
CD2
CD1
CG1
CG2
CE
A209 D210 T211 V212 A213 P214 V215 S216 Q217 H218 A219 I220 P221 F222 Y223 Q224 N225 L226 P227 S228 T229 T230 P231 K232 V233 Y234 V235 E236 L237 C238 N239 A240 S241 H242 I243 A244 P245 N246 S247 N248 N249 A250 A251 I252 S253 V254 Y255 T256 I257 S258 W259 M260 K261 L262 W263 V264 D265 N266 D267 T268 R269 Y270 R271 Q272 F273 L274 C275 N276 V277 N278 D279 P280 A281 L282 C283 D284 F285 R286 T287 N288 N289 R290 H291 C292 Q293
H/N
C
CA
CB
CD
CG
CD2
CD1
CG1
CG2
CE

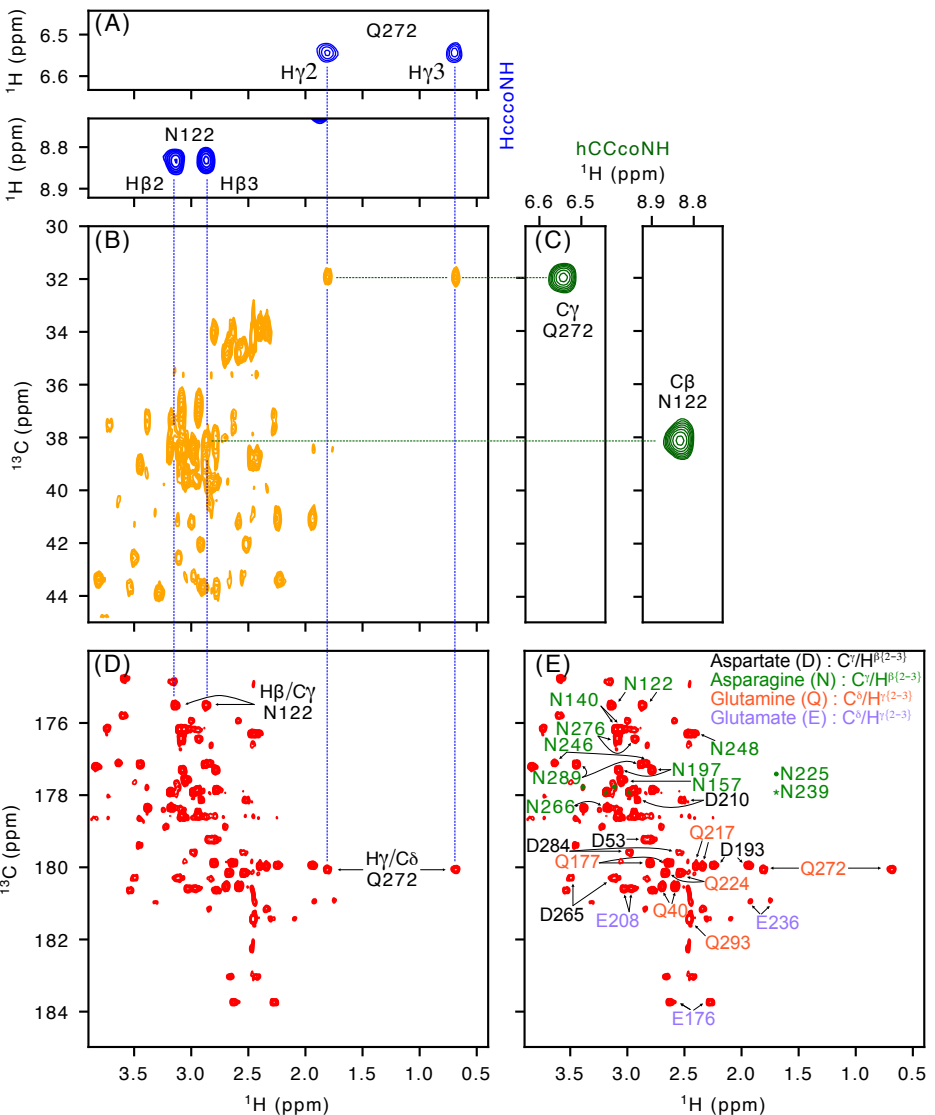
(A)
Q272
Hγ2
Hγ3
HcccoNH
N122
Hβ2
Hβ3
hCCcoNH
(B)
(C)
Cγ
Q272
Cβ
N122
(D)
Hβ/Cγ
N122
Hγ/Cδ
Q272
(E)
Aspartate (D) : Cγ/Hβ{2−3}
Asparagine (N) : Cγ/Hβ{2−3}
Glutamine (Q) : Cδ/Hγ{2−3}
Glutamate (E) : Cδ/Hγ{2−3}
N122
N140
N276
N246
N248
N197
N289
N157
N225
N239
N266
D210
Q217
D284
D53
D193
Q177
Q272
Q224
D265
E208
Q40
E236
Q293
E176
1H (ppm)
13C (ppm)

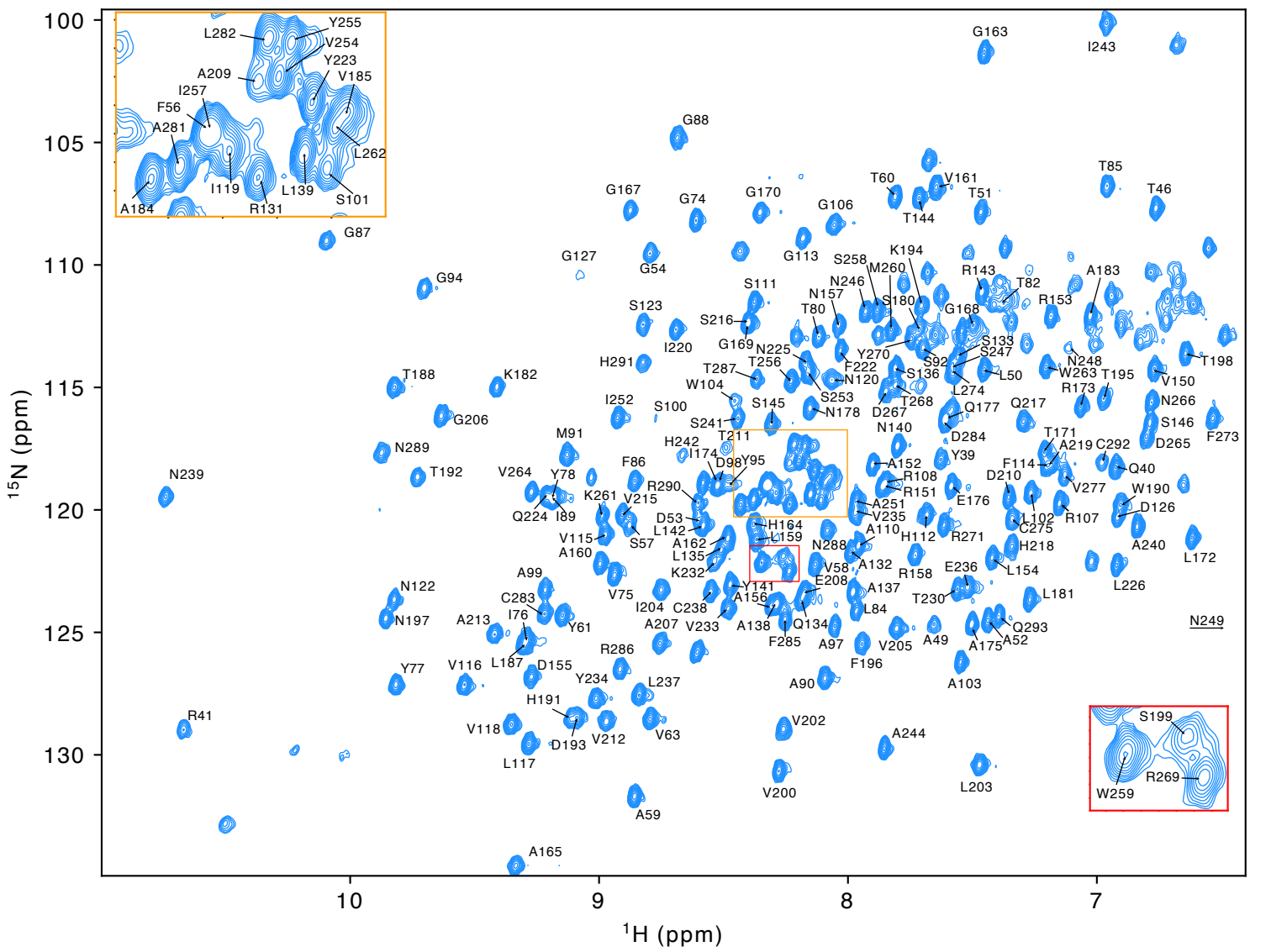

100
105
110
115
120
125
130
^{15}N (ppm)
10
9
8
7
^{1}H (ppm)
L282
Y255
V254
Y223
A209
V185
I257
F56
A281
L262
I119
L139
S101
A184
R131
G163
I243
G88
T85
T60
V161
T46
G167
G74
G170
G106
T51
T144
G87
G127
G54
G113
S258
K194
M260
R143
A183
G94
S111
N246
T82
N157
S180
R153
S123
T80
G168
S216
S133
I220
G169
N225
Y270
S247
H291
T256
F222
S92
N248
T198
T287
N120
S136
L50
W263
T195
T188
K182
W104
S253
T268
L274
R173
V150
I252
S100
S145
N178
D267
Q177
Q217
N266
G206
S241
N140
S146
M91
T211
D284
T171
F273
H242
A219
C292
D265
N289
I174
Y39
F114
Q40
F86
D98
Y95
A152
N239
T192
V264
Y78
R108
D210
R290
R151
V277
W190
K261
V215
A251
E176
D126
Q224
I89
D53
V235
L102
R107
H164
L142
A110
C275
V115
L159
H112
R271
A240
A160
S57
A162
N288
H218
L135
A132
L172
K232
V58
R158
E236
L154
A99
E208
Y141
A137
L226
N122
V75
A156
T230
L181
C283
I204
C238
L84
N197
A213
I76
Y61
A207
V233
A138
Q134
Q293
N249
F285
A97
V205
A49
A175
A52
R286
L187
D155
F196
Y77
V116
Y234
L237
A90
A103
H191
R41
V202
S199
V118
V212
V63
A244
D193
L117
R269
L203
V200
W259
A59
A165